

Stochastic Design Optimization of Microstructures with Utilization of a Linear Solver

Pınar Acar*, Siddhartha Srivastava[†] and Veera Sundararaghavan[‡]

University of Michigan, Ann Arbor, 48109, MI, USA

Microstructure design can have a substantial effect on the performance of critical components in numerous aerospace applications. However, the stochastic nature of metallic microstructures leads to deviations in material properties from the design point, and alters the performance of these critical components. In this work, an inverse stochastic design approach is introduced such that the material is optimized while accounting for the inherent variations in the microstructure. The highlight is an analytical uncertainty quantification model via a Gaussian distribution to model propagation of microstructural uncertainties to the properties. Metallic microstructure is represented using a finite element discretized form of the orientation distribution function. A stochastic optimization approach is proposed that employs the analytical model for uncertainty quantification, to explore to maximize the yield strength of Galfenol microstructure in a compliant beam when constrained by uncertainties in the designed natural frequency of vibration. The results of the stochastic optimization approach are validated using Monte Carlo Simulation (MCS). We also show that multiple microstructure solutions can be identified using the null space of the linear systems involved in the optimization.

I. Introduction

Microstructural uncertainties arise from variations in manufacturing process conditions and can affect the performance of metallic materials in aerospace components. This is an aleatoric uncertainty, is unavoidable and is naturally present in metallic systems. The present work aims to investigate the effect of aleatory uncertainties in microstructure modeling and inverse design of stochastic microstructural features to achieve a prescribed statistical range of engineering properties. Current state of the art only addresses the direct uncertainty quantification problem (effect of uncertain microstructures on properties) and the stochastic inverse problem has not been addressed to the best of our knowledge. The direct problem has been generally addressed using computational techniques such as Monte Carlo simulation (MCS), collocation and spectral decomposition methods. Huyse and Maes¹ studied the effect of microstructural uncertainties on homogenized parameters by using random windows from the real microstructure, and performed MCS to identify the stochasticity in elastic parameters such as Young's modulus and Poisson's ratio. Sakata et. al² showed the variations in Young's modulus and Poisson's ratio due to microscopic uncertainties. They validated the results of their perturbation-based homogenization method with MCS. In another paper, Sakata et. al³ implemented a Kriging approach to calculate the probability density functions of the material properties, and used MCS to study the uncertainties in geometry and material properties of a microstructure through the same perturbation-based homogenization method. A computational stochastic modeling approach for random microstructure geometry was presented by Clement et. al.^{4,5} The authors presented a high dimensional problem due to the high number of stochastic variables to represent the microstructure geometry. This high dimensionality was reduced with implementation of Polynomial Chaos Expansion (PCE). Creuziger et. al⁶ examined the uncertainties in the orientation distribution function (ODF) values of a microstructure due to the variations in the pole figure (PF) values by using MCS. Juan et. al⁷ used MCS to study effects of sampling strategy on the determination of various characteristic microstructure parameters such as grain size distribution and grain topology distribution. Hiriyur et. al⁸ studied an extended finite element method

*Graduate Research Assistant, Department of Aerospace Engineering, AIAA Student Member.

[†]Graduate Research Assistant, Department of Aerospace Engineering

[‡]Associate Professor, Department of Aerospace Engineering, AIAA Senior Member.

(XFEM) coupled with an MCS approach to quantify the uncertainties in the homogenized effective elastic properties of multiphase materials. The uncertain parameters were assumed to be aspect ratios, spatial distribution and orientation. They used a strain energy approach to analyze the uncertainties of in-plane Young’s modulus and Poisson’s ratio. Kouchmeshky and Zabarás⁹ presented propagation of initial texture and deformation process uncertainties on the final product properties. They used a data-driven approach to identify the joint probability distributions of random variables with Maximum Entropy Method, and modeled the stochastic problem using a stochastic collocation approach. Madrid et. al¹⁰ examined the variability and sensitivity of in-plane Young’s modulus of thin nickel polycrystalline films due to uncertainties in microstructure geometry, crystallographic texture, and numerical values of single crystal elastic constants by using a numerical spectral technique. Niezgodá et. al¹¹ computed the variances of the microstructure properties by defining a stochastic process to represent the microstructure. They marked the sensitive regions in the convex hull generated with Principal Component Analysis (PCA), and calculated the probability distributions of stiffness and yield stress in case of low, medium and high variances.

These numerical uncertainty quantification techniques studied in literature require high computational costs since they represent the joint probability distributions of the random variables either using interpolation functions or samples. As the problem complexity or the number of variables increases the number of interpolation terms or sample points also increase. This is especially true for the ODFs which are discretized using finite element nodes or spectral basis, and contain large number of free parameters whose joint distribution needs to be sampled. Another drawback of the computational methods is the difficulty of satisfying design constraints such as volume fraction normalization. All these disadvantages imply the necessity of developing analytical solutions as a first step in uncertainty quantification. In this work, we present an analytical formulation based on a Gaussian distribution approach to represent the variations of the random parameters. The variations of in-plane Young’s modulus (E_1) and shear modulus (G_{12}) are assumed to be provided by the manufacturer, and consistent with the Gaussian distribution. Then the probability distributions of the ODFs are computed by solving an inverse problem. The variations in the compliance parameters, S_{11} and S_{66} , are found first with transformation of random variables rule using input variations in E_1 and G_{12} . The compliance parameters are calculated first since they can be represented with linear equations in terms of the ODFs. The probability distributions of the compliance parameters are also assumed to be modeled with a Gaussian approach despite their nonlinear relation to E_1 and G_{12} since the input uncertainties are very small. Then the inverse problem to find the statistical properties of the ODFs is defined as a linear programming (LP) problem. A global stochastic optimization approach is implemented to this analytical solution framework to maximize the yield stress under vibration tuning constraints defined for the first bending and torsion natural frequencies of the cantilever beam. The optimization variables are defined as the in-plane Young’s modulus (E_1) and shear modulus (G_{12}) of the Galfenol material, and each design sample is assumed to have the same level of uncertainty. The LP problem approach has been studied before by the authors to find the optimal processing route to produce a optimum microstructure design to the same vibration tuning problem.¹² However, the LP approach presented before was for the ODF solution of a deterministic system.¹²⁻¹⁴ In this paper, we extend the LP solution methodology to identify the statistical parameters of the ODFs in case of uncertainties in material properties. To the best of the authors’ knowledge this is the first analytical effort in literature for quantification of microstructural stochasticity given the desired statistical range in properties, in effect, a stochastic inverse problem for microstructure design. The optimization results are also compared to the results of computational methods which employ MCS to quantify the uncertainties. The analytical algorithm is able to compute the same optimization variables and a very close objective function value to the MCS solution, and while decreasing the computational time by almost two orders of magnitude. Once the optimum ODFs are achieved, then the multiple solution directions are identified using the direct linear solver, which was presented in our earlier works.¹²⁻¹⁴ The linear solver is capable of finding exact solutions for multiple and infinite solution problems. The effect of uncertainties on the design objective is also discussed at the end by comparing the optimum results with the deterministic solution for maximum yield stress. The organization of the paper is as follows: Section II addresses multi-scale modeling of microstructures, particularly the computation of volume-averaged properties. We introduce the analytical model for uncertainty quantification and stochastic optimization approach in Section III. In Section IV, we report the results of the stochastic optimization studies performed using the analytical model and MCS to quantify the uncertainties. A summary of the paper with potential future applications is presented in Section V.

II. Multi-Scale Modeling of Microstructures

The alloy microstructure consists of multiple crystals with each crystal having an orientation. The generalized Hooke's law for the aggregate of crystals may be written in the form:

$$\langle \epsilon_{ij} \rangle = \mathbf{S}^{eff} \langle \sigma_{kl} \rangle, \quad (1)$$

where $\langle \epsilon_{ij} \rangle$ and $\langle \sigma_{kl} \rangle$ are the volume-averaged strain and stress respectively, \mathbf{S}^{eff} is the effective compliance tensor in the coordinate system of the part. Assuming homogeneity of the deformation in a macroscale elementary volume, the effective elastic properties may be found through averaging using the Taylor approximation:¹⁵

$$\mathbf{S}^{eff} = \langle \mathbf{S} \rangle, \quad (2)$$

If the effect of factors (e.g. crystal size and shape) is ignored, averaging (denoted by $\langle \cdot \rangle$ in the equation above) can be performed over the ODF (represented by \mathbf{A}). The ODF gives the volume density of each orientation in the microstructure. If the orientation-dependent property for single crystals, $\chi(r)$, is known, any polycrystal property can be expressed as an expected value, or average, given by:

$$\langle \chi \rangle = \int_{\mathbf{R}} \chi(r) \mathbf{A}(r, t) dv, \quad (3)$$

where ODF, \mathbf{A} , is a function of orientation r , and time t (for plasticity problems). The average value is computed by integrating in the representative volume element, dv , which can be obtained by considering the crystallographic symmetries.

The present work employs the axis-angle parameterization of the orientation space proposed by Rodrigues¹⁶ since angle-axis representations define an alternate way of representing orientations compared to Euler angles.^{17,18} The Rodrigues' parameterization is created by scaling the axis of rotation n as $r = n \tan(\frac{\theta}{2})$, where θ is the rotation angle. Finite element discretization of the orientation space and associated integration schemes using Gauss quadrature allows matrix representation of Eq. 3. The ODF is discretized into N independent nodes with N_{elem} finite elements and N_{int} integration points per element. Using this parameterization, any polycrystal property can be expressed in a linear form as follows.¹⁹

$$\langle \chi \rangle = \int_{\mathbf{R}} \chi(r) \mathbf{A}(r, t) dv = \sum_{n=1}^{N_{elem}} \sum_{m=1}^{N_{int}} \int_{\mathbf{R}} \chi(r_m) \mathbf{A}(r_m) w_m |J_n| \frac{1}{(1 + r_m \cdot r_m)^2}, \quad (4)$$

where $A(r_m)$ is the value of the ODF at the m^{th} integration point with global coordinate r_m of the n^{th} element, $|J_n|$ is the Jacobian determinant of the n^{th} element, w_m is the integration weight associated with the m^{th} integration point, and $\frac{1}{(1+r_m \cdot r_m)^2}$ represents the metric of Rodrigues parameterization. This can be shown to be equivalent to an equation linear in the ODF: $\langle \chi \rangle = \mathbf{p}^T \mathbf{A}$, where \mathbf{A} is a vector containing the ODF values at the k independent nodes of the ODF mesh.²⁰ In addition, the ODF is normalized to unity as $\mathbf{q}^T \mathbf{A} = 1$ where \mathbf{q} is a normalization vector.

The polycrystal compliance, $\bar{\mathbf{S}}$, is computed through a weighted average (over \mathbf{A}) of the compliance values of individual crystals expressed in the sample reference frame using the lower bound approach (Reuss average). The yield stress is computed using a crystal plasticity model from our recent work.²¹ The ODF representation for Body Centred Cubic (BCC) Galfenol material is shown in Fig. 1.

III. Stochastic Design Optimization of Microstructures

A. Problem Definition: Vibration Tuning for a Galfenol Beam

The optimization problem studied in this paper aims to find the optimum microstructure design to maximize the yield stress of a cantilever beam made of Galfenol under vibration tuning constraints (Fig. 2). The material properties of the Galfenol beam are computed with the ODF values at independent nodal points. The same optimization problem was presented before¹²⁻¹⁴ in case of deterministic design variables. The vibration tuning constraints are defined for the first natural bending and torsion frequencies of the beam, which can be formalized in terms of Young's modulus (E_1) and shear modulus (G_{12}) for an orthotropic material.

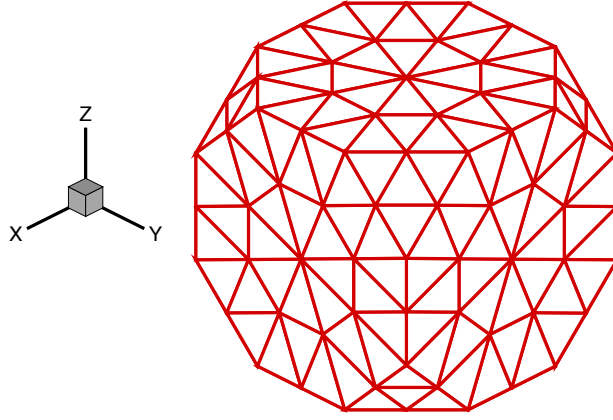


Figure 1. ODF representation in the Rodrigues fundamental region for cubic crystal symmetry

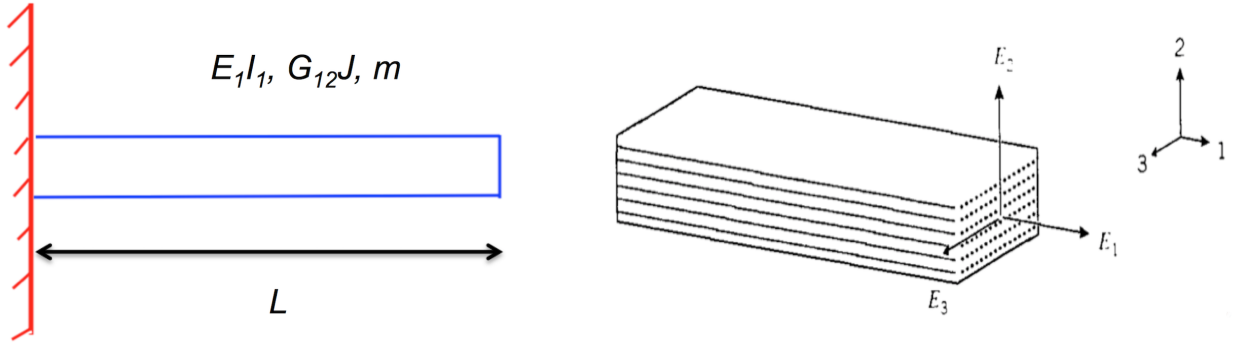


Figure 2. Geometric representation of Galfenol beam vibration problem

$$\omega_{1t} = \frac{\pi}{2L} \sqrt{\frac{G_{12}J}{\rho I_p}} \quad (5)$$

$$\omega_{1b} = (\alpha L)^2 \sqrt{\frac{E_1 I_1}{m L^4}} \quad \text{and} \quad \alpha L = 1.87510, \quad (6)$$

where $G_{12} = 1/S_{66}$, $E_1 = 1/S_{11}$, and S_{11} and S_{66} being the compliance elements. In these formulations, J is torsion constant, ρ is density, I_p is polar inertia moment, m is unit mass, L is length of the beam and I_1 is moment of inertia along axis-1. To solve the problem, the length of the beam is taken as $L = 0.45$ m and the beam is considered to have a rectangular cross-section with dimensions $a = 20$ mm and $b = 3$ mm.

B. Analytical Model for Uncertainty Quantification

The stochastic optimization approach presented in this work for vibration tuning of a Galfenol beam microstructure starts with an assumption that we are given the variations of E_1 and G_{12} parameters. According to this assumption, both E_1 and G_{12} vary $\pm 5\%$ around their mean values with respect to Gaussian distribution. The uncertainties of the ODFs are identified through an inverse design LP problem since the compliances, S_{11} and S_{66} , can be defined with linear equations in terms of the ODFs using a lower bound average. However, the relation between the compliances and input parameters is nonlinear since $S_{11} = 1/E_1$ and $S_{66} = 1/G_{12}$. Similarly the variables for the vibration tuning constraints, the first torsion natural frequency (ω_{1t}) and the first bending natural frequency (ω_{1b}), are nonlinear in terms of the input variables. The transformation of random variables rule is used to identify the statistical properties for S_{11} , S_{66} , ω_{1t}

and ω_{1b} . Once the probability distributions of S_{11} and S_{66} are identified the uncertainties in the ODF values are calculated using linear transformation. We assume that the probability distributions of the compliance parameters can be modeled with a Gaussian distribution approximation since the variations in the Gaussian input parameters (E_1 and G_{12}) are small. The analytical modeling approaches used for computing linear and nonlinear material properties are summarized in the next sections.

1. Uncertainties in linear material properties

The uncertainties in the linear material properties are computed using Gaussian distribution features in linear relations. The summary of the Gaussian approach to model a linear property is given below: Assume a d -dimensional multivariate Gaussian distribution: $\mathbf{X} \sim \mathcal{N}_d(\boldsymbol{\mu}, \boldsymbol{\Sigma})$. Now we define a new random variable:

$$\mathbf{Z} = \mathbf{C}\mathbf{X} \quad (7)$$

where \mathbf{C} is a constant matrix. Then, \mathbf{Z} is also Gaussian distributed.²⁰ The mean vector and covariance matrix of \mathbf{Z} are given by:

$$\boldsymbol{\mu}_Z = \mathbf{C}\boldsymbol{\mu}_X \quad (8)$$

$$\boldsymbol{\Sigma}_Z = \mathbf{C}\boldsymbol{\Sigma}_X\mathbf{C}^T \quad (9)$$

The Gaussian approach presented here can be modified accordingly to represent the variations in the ODFs and linear material properties. Since the ODF values are identified from an inverse problem we assume that the first $k-1$ number of ODFs are independent (where k indicates the total number of ODF variables at independent nodes) to decrease the amount of random variables. In order to satisfy the unit volume fraction constraint, the equations to compute the statistical properties of the k^{th} ODF are modified. The mean and variance of the k^{th} ODF value can be obtained as $\mathbf{E}[\mathbf{A}_k] = \mathbf{c}^T\boldsymbol{\mu}_A + \frac{1}{q_k}$ and $\sigma^2[\mathbf{A}_k] = \mathbf{c}^T\boldsymbol{\Sigma}_A\mathbf{c}$, where $c_i = -\frac{q_i}{q_k}$, $\boldsymbol{\mu}_A = E(A_i)$ and $\boldsymbol{\Sigma}_A = E[(A_i - \mu_{A_i})(A_j - \mu_{A_j})]$. After the modification for the k^{th} variable, the ODF covariance matrix can be written as:

$$\boldsymbol{\Sigma}_A = \begin{bmatrix} \boldsymbol{\Sigma}_A^* & \mathbf{S} \\ \mathbf{S}^T & \sigma_k^2 \end{bmatrix} \quad (10)$$

where, $\boldsymbol{\Sigma}_A^*$ is the covariance matrix defined for the first independent $k-1$ ODFs, and \mathbf{S} is a column vector whose values are given by:

$$\mathbf{S}_i = -\frac{1}{q_k} \sum_{j=1}^{k-1} q_j (\boldsymbol{\Sigma}_A^*)_{ij} \quad (11)$$

The uncertainties in the linear material properties are computed using the linear transformation. The linear variables chosen for this study are the compliance parameters, S_{11} and S_{66} . The mean and variance equations for S_{11} can be shown as below using the Gaussian approach. The same computation also applies to the statistical parameters of S_{66} .

$$\boldsymbol{\mu}_{S_{11}} = \mathbf{p}_1^T \boldsymbol{\mu}_A \quad (12)$$

$$\sigma_{S_{11}}^2 = \mathbf{p}_1 \boldsymbol{\Sigma}_A \mathbf{p}_1^T \quad (13)$$

where \mathbf{p}_1 represents the single crystal property values for \mathbf{S}_{11} .

2. Uncertainties in nonlinear material properties

The uncertainties in nonlinear material properties are computed using the transformation of random variables rule. The application of this rule is as follows: Given the input parameter, x , and the output parameter, y , we assume that the relation between x and y can be identified using $y = h(x)$, and can be inverted as $x = u(y)$. This method computes a Jacobian value, J , based on this explicit relation (where $J = du/dy$),

and finds the probability density function (PDF) of the output variable as a product of input PDF and the Jacobian. Eq. 14 shows the computation of output PDF:

$$f_y(y) = f_x[u(y)] \times |J| \quad (14)$$

where f_x and f_y are the PDFs of input and output variables respectively. Since the input PDF, f_x , and inverted function, $u(y)$ are already known, the output PDF, f_y , can be computed using this method. Then, the expected value, $E[y]$, and variance, σ_y^2 , of the output parameter can be calculated using Eq. 15 and 16 respectively:²²

$$E[y] = \int_{y_{min}}^{y_{max}} y f_y(y) dy \quad (15)$$

$$\sigma_y^2 = E[(y - E[y])^2] \quad (16)$$

where y_{min} and y_{max} are the minimum and maximum values of the output variable, y , can take. These values can be computed using the relation $y = h(x)$ for the minimum and maximum values of the input variable, x_{min} and x_{max} , respectively. The approach is first applied to compute the PDF of the compliance parameters, $S_{11} = 1/E_1$ and $S_{66} = 1/G_{12}$. The same method is then used to compute the PDFs of the first torsion and bending natural frequencies of a cantilever beam, ω_{1t} and ω_{1b} , using Eq. 5 and Eq. 6.

C. Linear programming approach for inverse design

The statistical properties of the ODF values are identified by solving the inverse design problem as an LP problem. The PDFs of S_{11} and S_{66} were previously computed using the transformation of the random variables rule. The mean values and variances of S_{11} and S_{66} were then computed using Eq. 15 and Eq. 16. The variations in these parameters were assumed to agree with the Gaussian distribution due to small variations in the input parameters, E_1 and G_{12} . With this assumption the ODF values can be determined by solving an LP problem. A general formulation of an LP problem is given as follows:

$$\begin{aligned} & \min \mathbf{f}^T \mathbf{x} \\ & \text{such that } \mathbf{A}_{eq} \mathbf{x} = \mathbf{b}_{eq} \\ & \quad \mathbf{A} \mathbf{x} \leq \mathbf{b} \\ & \quad \mathbf{lb} \leq \mathbf{x} \leq \mathbf{ub} \end{aligned}$$

The unknown vector, \mathbf{x} , of this LP problem includes the mean values and variances of the first $k - 1$ ODF values: $\boldsymbol{\mu}_A$ and $\boldsymbol{\sigma}_A^2$. The mean and variance terms related to the k^{th} ODF value can then be obtained using the definitions for $\boldsymbol{\mu}_A$ and $\boldsymbol{\sigma}_A^2$ in the volume fraction normalization constraint equation. The equality constraints are derived by using the homogenized linear equations for the mean values (Eq.17 and Eq. 18) and variances (Eq. 19 and Eq. 20):

$$\mathbf{p}_1^T \boldsymbol{\mu}_A = \mu_{S_{11}} \quad (17)$$

$$\mathbf{p}_6^T \boldsymbol{\mu}_A = \mu_{S_{66}} \quad (18)$$

$$\mathbf{p}_1 \boldsymbol{\Sigma}_A \mathbf{p}_1^T = \sigma_{S_{11}}^2 \quad (19)$$

$$\mathbf{p}_6 \boldsymbol{\Sigma}_A \mathbf{p}_6^T = \sigma_{S_{66}}^2 \quad (20)$$

In these equations, \mathbf{p}_1 and \mathbf{p}_6 are the vectors of length k including single crystal coefficient values for S_{11} and S_{66} respectively, $\mu_{S_{11}}$ and $\mu_{S_{66}}$ are the mean values, and $\sigma_{S_{11}}^2$ and $\sigma_{S_{66}}^2$ are variances of S_{11} and S_{66} .

Accounting for the normalization constraint, we only solve for the $k-1$ ODF values. The augmented system of the equality constraints for the first $k-1$ ODF values can be derived as:

$$\begin{bmatrix} [p_1^T - \frac{p_1(k)}{q_k} q^T]_{1 \times (k-1)} & \mathbf{0}_{1 \times (k-1)} \\ [p_6^T - \frac{p_6(k)}{q_k} q^T]_{1 \times (k-1)} & \mathbf{0}_{1 \times (k-1)} \\ \mathbf{0}_{1 \times (k-1)} & P_{1 \times (k-1)}^* \\ \mathbf{0}_{1 \times (k-1)} & P_{6 \times (k-1)}^* \end{bmatrix} \begin{bmatrix} \mu_{A(k-1) \times 1} \\ \sigma_{A^2(k-1) \times 1} \end{bmatrix} = \begin{bmatrix} \mu_{S_{11}} - \frac{p_1(k)}{q_k} \\ \mu_{S_{66}} - \frac{p_6(k)}{q_k} \\ \sigma_{S_{11}}^2 \\ \sigma_{S_{66}}^2 \end{bmatrix}$$

where \mathbf{q} is a vector containing the first $k-1$ values of the normalization vector, and $\mathbf{0}_{1 \times (k-1)}$ is a row vector of zeros with a length of $k-1$. The elements of the rows vectors, P_1^* and P_6^* , can be calculated as below by using Eq. 19 and Eq. 20 with the definition for Σ_A ($i = 1, 2, \dots, k-1$):

$$P_1^*(i) = [p_1^2(i) + (p_1(k) + 1)(p_1(i)c(i)) + (p_1^2(k)c^2(i))] \quad (21)$$

$$P_6^*(i) = [p_6^2(i) + (p_6(k) + 1)(p_6(i)c(i)) + (p_6^2(k)c^2(i))] \quad (22)$$

The first inequality equation is derived for the lower boundary of the k^{th} ODF value such that the first $k-1$ ODFs should satisfy the constraint, $\mathbf{q}^T \mu_A \leq 1$, to guarantee that the unit volume normalization constraint is satisfied with a non-negative k^{th} ODF value ($\mathbf{q} > \mathbf{0}$ and $q_k > 0$). Since the compliance parameters are assumed to agree with the Gaussian approach the ODF values have the same distribution because of their linear relation. We used the following inequalities to ensure that the probability distributions of the ODFs always satisfy the non-negativity condition: $-\mu_A + z\sigma_{A^2} \leq \mathbf{0}$ and $-\mu_{A_k} + z\sigma_{A_k}^2 \leq \mathbf{0}$ where z is a constant to be determined. In these inequality equations the standard deviation parameter is approximated by the variance since the variances are the unknowns in the LP problem definition. The standard deviation can be replaced with the variance since the standard deviation and variance values of the compliances are in the same order, and the ODFs are assumed to follow the same trend. However, the variances are controlled with the constant parameter, z , rather than directly considering the traditional 3.5σ assumption for Gaussian distribution. The inequality equation for the variation of the k^{th} ODF can be manipulated further by using the definitions for μ_{A_k} and $\sigma_{A_k}^2$. The final form of the inequality equations is given in Eq. 23, 24 and 25:

$$\mathbf{q}^T \mu_A \leq 1 \quad (23)$$

$$-\mu_A + z\sigma_{A^2} \leq \mathbf{0} \quad (24)$$

$$-\frac{1}{q_k} \mathbf{q}^T \mu_A + zC^* \sigma_{A^2} \leq \frac{1}{q_k} \quad (25)$$

where the elements of the C^* vector are: $C^*(i) = c(i)^2$. Using Eq. 23, 24 and 25 the augmented system for the inequality constraints can be derived as below:

$$\begin{bmatrix} \mathbf{q}^T_{1 \times (k-1)} & \mathbf{0}_{1 \times (k-1)} \\ -[I]_{(k-1) \times (k-1)} & z[I]_{(k-1) \times (k-1)} \\ \frac{1}{q_k} \mathbf{q}^T_{1 \times (k-1)} & zC^*_{1 \times (k-1)} \end{bmatrix} \begin{bmatrix} \mu_{A(k-1) \times 1} \\ \sigma_{A^2(k-1) \times 1} \end{bmatrix} \leq \begin{bmatrix} 1 \\ \mathbf{0}_{(k-1) \times 1} \\ \frac{1}{q_k} \end{bmatrix}$$

where $[I]$ is the identity matrix. The objective of the stochastic optimization problem is to maximize the mean yield stress value of the beam. Since the standard LP problem defines the objective function for minimization instead of maximization the negative of the yield stress value, $-\sigma_y$, is minimized. This objective function is also linear in the ODFs such that: $-\sigma_y = (-\mathbf{y}^T + (\frac{y_k}{q_k})\mathbf{q}^T)\mu_A - \frac{y_k}{q_k}$ where \mathbf{y} is the vector of yield stress coefficients for the first $k-1$ single crystals and y_k is the same coefficient value for the k^{th} single crystal. The objective function, f is defined as: $\mathbf{f} = (-\mathbf{y}^T + (\frac{y_k}{q_k})\mathbf{q}^T)\mu_A$ and therefore: $-\sigma_y = f - \frac{y_k}{q_k}$. The objective function of the LP problem for min $\mathbf{f}^T \mathbf{x}$, can be written as:

$$\mathbf{f} = [\mathbf{y}_{1 \times (k-1)}^* \mathbf{0}_{1 \times (k-1)}]^T \quad (26)$$

where \mathbf{y}^{*T} is defined as: $\mathbf{y}^{*T} = -\mathbf{y}^T + \left(\frac{y_k}{q_k}\right)\mathbf{q}^T$. In the final step, the lower and upper bounds are determined considering the non-negativity conditions for the ODFs. The unknowns of the LP problem, the mean values and on-diagonal variance terms of the ODF parameters, have a zero value lower bound. An ODF, A_i , can have the value of $1/q_i$ as an upper bound. This is also true for the mean values, μ_{A_i} . However, the variances are known to be lower than the mean values in this problem. Therefore defining the same upper bound values for the corresponding variance terms is mathematically possible. The lower and upper bound vectors for this problem are then defined as: $\mathbf{lb} = [\mathbf{0}_{1 \times 2(k-1)}]$ and $\mathbf{ub} = [1/q_i \ 1/q_i]$, where $i = 1, 2, \dots, k - 1$.

D. Definition of the stochastic optimization problem

The stochastic optimization problem for the vibration tuning of a Galfenol beam microstructure with yield stress objective is defined with the implementation of the presented analytical solution methodology for uncertainty quantification. The optimization starts with the global sampling for the input variables, μ_{E_1} and $\mu_{G_{12}}$, which are the mean values of E_1 and G_{12} . In the next step, the statistical properties of compliances, S_{11} and S_{66} , and natural frequencies, ω_{1t} and ω_{1b} , are calculated using the random variables transformation rule in Section III-B2. The ODF solution satisfying the calculated statistical properties of the compliances and maximizing the mean yield stress value is identified by implementing the LP problem of Section III-C to the optimization algorithm. The mathematical formulation of the optimization problem is given below:

$$\max \mu_{\sigma_y} \quad (27)$$

$$\text{subject to } P(20.25 \text{ Hz} \leq \omega_{1t} \leq 24.25 \text{ Hz}) = 1 \quad (28)$$

$$\text{subject to } P(132.75 \text{ Hz} \leq \omega_{1b} \leq 139.75 \text{ Hz}) = 1 \quad (29)$$

$$\mathbf{s} = (\mu_{E_1}, \mu_{G_{12}}), \quad (30)$$

where the optimization variables are μ_{E_1} and $\mu_{G_{12}}$ in the global problem, and the means and variances of the first $k - 1$ ODFs in the LP problem definition. Eq. 27 shows the objective function, which is determined as maximization of the mean yield stress value. The output variables have probability distributions based on their statistical properties. The constraint parameters are expected to satisfy the strict vibration tuning constraints in every point of their probability distribution. Therefore the probability of satisfying the design constraints is expected to be 1 as shown in Eq. 28 and Eq. 29. In the last row, \mathbf{s} shows the vector of global optimization variables. The corresponding ODF solution to the optimum values of the global variables provides the optimal microstructure design of the problem. The non-negativity condition of the ODFs is considered as a lower bound in the LP problem. The volume normalization constraint is also considered through the definition of the k^{th} ODF and the inequality constraint in Eq. 23.

1. Multiple solutions with a direct linear solver

After the computation of one optimum design, the multiple optimum ODF solutions to the Galfenol problem are identified with the implementation of a direct linear solver through the use of linear parameters. These linear parameters are the optimum values of the compliance parameters and yield stress of the orthotropic Galfenol beam, which can be computed through the optimum ODFs using the equations below:

$$\langle S^* \rangle = \int S A^* dV \quad (31)$$

$$\langle \sigma_y^* \rangle = \int \sigma_y A^* dV \quad (32)$$

In Eq. 31 and 32, S^* and σ_y^* are the optimum values for the compliance parameters and yield stress respectively, \mathbf{A}^* denotes the vector of optimum ODF values. The objective of this step is to identify all the ODFs which provide the same S^* and σ_y^* values. The direct linear solver determines the multiple ODFs for the optimum properties. The solver is capable of finding multiple/infinite solutions because it uses null space of the coefficient matrix to find the directions of the solutions. The use of the null space approach requires any one solution to the problem. This one solution comes from the global optimization result for this problem. The remaining infinite solutions are defined as the sums of this one solution and solution

directions represented by null space vectors. The coefficient matrix can be defined using the linear relations for macro properties and the unit volume fraction constraint for the ODF. The size of the coefficient matrix is $(4 \times k)$ because the rows are representing 3 independent linear equations for S_{11} , S_{66} and σ_y calculation, and one design constraint for volume fraction normalization ($\int \mathbf{A}d\mathbf{V} = \mathbf{1}$). Assuming \mathbf{C} is the coefficient matrix including the entries for compliances, S , and yield stress, σ_y , the infinite solutions can be represented as shown next ($i = 1, 2, 3, 4, \dots, n$):

$$\mathbf{A}_i = \mathbf{A}_1 + \lambda \mathbf{V}_i; \quad (33)$$

$$\mathbf{V}_i = \text{Null}(\mathbf{C}(:, i)) \quad (34)$$

where Eq. 33 defines the infinite solutions, \mathbf{A}_i , using one solution, \mathbf{A}_1 , and null space vectors, \mathbf{V}_i . n is the number of null space vectors. Even though the number of null space vectors is finite, the number of solutions can be infinite because λ can be any number that satisfies the ODF positiveness constraint ($\mathbf{A} \geq \mathbf{0}$). Because the optimization problem is solved in the space of macro properties (property closure of homogenized parameters), and the space of macro properties is generated by the ODF values through averaging equations, any point inside this solution domain corresponds to a known set of ODF values. Therefore, there is always at least one optimal ODF solution inside this domain. The solution strategy aims to find this optimum solution not only when it is unique but also when it is multiple. A more detailed discussion about implementation of the linear solver and generation of the property hulls can be found in the earlier papers of the authors'.¹²⁻¹⁴

IV. Results

The stochastic optimization is performed using Incremental Space Filler (ISF) as the global sampling method for the input parameters, and Non-Dominated Sorting Genetic Algorithm (NSGA-II) as the optimization algorithm in Modefrontier software. The same sampling and optimization algorithm were used in the previous deterministic optimization studies.^{12,13} However, the limits of the design constraints are changed in this problem. In order to compare the effect of uncertainty to the final design and material properties we also performed a deterministic optimization for the same problem. The constant parameter, z , of the analytical LP approach is considered as $z = 3.5$. In addition we also performed another stochastic optimization using MCS method to model the uncertainties. In this MCS technique, we used 10000 samples to generate the probability distributions for one set of global ISF sample points. The compliance values, S_{11} and S_{66} , are calculated using the exact equations in terms of the input parameters. Then the ODF solutions are identified by solving for 10000 separate LP problems per one global sample. These deterministic LP problems are simplified forms of the presented LP methodology since they do not consider the inequality constraints defined for the variations (Eq. 24 and Eq. 25). The MCS method, despite the use of the LP approach to solve the ODFs, is a computational burden compared to the required computational time to run the analytical solution. The optimum design parameters of stochastic optimization studies are given in Table 1. In all cases, the optimum parameters correspond to multiple optimal polycrystal designs with the implementation of the direct linear solver. The optimum deterministic parameters are also shown as the best case (with no uncertainties) in Table 1 to indicate the significant impact of the uncertainties to the design objective. The significant difference between the computational times spent on the stochastic optimization studies is also pointed in the last row of Table 1.

The difference between the optimum objective function values of the best case and stochastic optimization (Table 1) implies the substantial impact of the input uncertainties to the engineering properties. One critical feature of the results is that both stochastic optimization applications were able to identify the same solution for the global input parameters, μ_{E_1} and $\mu_{G_{12}}$. However, the optimum design criteria and objective function values are slightly different due to the different solution approaches in the analytical model such as random variables transformation rule and extended LP problem implementation by consideration of the ODF variances in contrast to the exact solution formulas being used by the MCS method. The variations of the yield stress and vibration frequencies of the stochastic optimum designs are shown in Fig. 3. According to the results in Fig. 3 the analytical model is able to capture the values and variances of the optimum material properties.

After identifying the optimum solutions to the stochastic problems the multiple polycrystal designs are also computed using the direct linear solution methodology with null space approach. Some of the multiple

Table 1. Stochastic Optimization Results for Vibration Tuning of the Galfenol Beam

Best Case	Stochastic (Analytical)	Stochastic (MCS)
$\sigma_y = 367.9385$ MPa	$\mu_{\sigma_y} = 340.1034$ MPa	$\mu_{\sigma_y} = 340.2584$ MPa
$\omega_{1t} = 22.7038$ Hz	$\mu_{\omega_{1t}} = 22.8272$ Hz	$\mu_{\omega_{1t}} = 22.7408$ Hz
$\omega_{1b} = 134.3167$ Hz	$\mu_{\omega_{1b}} = 136.4554$ Hz	$\mu_{\omega_{1b}} = 136.2892$ Hz
$E_1 = 262.5002$ GPa	$\mu_{E_1} = 270.3112$ GPa	$\mu_{E_1} = 270.3112$ GPa
$G_{12} = 87.5001$ GPa	$\mu_{G_{12}} = 87.8067$ GPa	$\mu_{G_{12}} = 87.8067$ GPa
$t = 5$ mins	$t = 20$ mins	$t = 44$ hours 35 mins

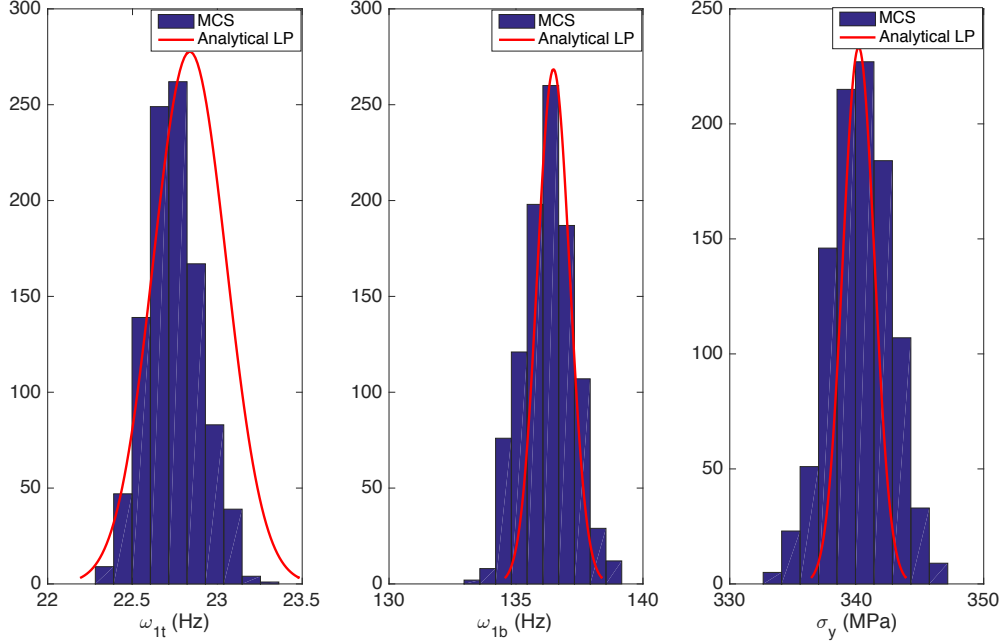


Figure 3. The variations of yield stress and vibration frequencies of the stochastic optimum designs

optimum solutions to the ODF mean values obtained by the analytical model and MCS are shown in Fig. 4. The first microstructure design of both solutions is the optimum initial design identified with the global optimization. The other microstructures are obtained using the same independent null space vectors in the direct linear solver for both analytical and MCS solutions.

The small differences between the analytical model and MCS results in the final material properties shown in Fig. 3 and multiple optimum ODF solutions shown in Fig. 4 can be explained with two features of the analytical approach. First, the analytical solution assumes that the first $k - 1$ ODFs are independent, and identifies only the on-diagonal variances for these ODFs. The system of equations in the LP problem already imply an underdetermined system, and the consideration of the non-diagonal terms makes the solution infeasible. However, the MCS method automatically considers the dependencies of the ODFs since it uses the exact solutions with direct sampling. The other reason is predicted to be the effect of the adjustable constant parameter, z , of the analytical solution, which represents the ODF variations. We used $z = 3.5$ in the results reported in Fig. 3 and Fig. 4. The effect of this parameter is further investigated by computing the yield stress values of the optimum microstructure using different z values. The same analysis is not performed for the natural frequency parameters since they are directly related to the global variables, not to the LP problem, so the change in z parameter does not affect them. The yield stress distributions of the optimum microstructure design with varying z values in the analytical solution are shown in Fig. 5.

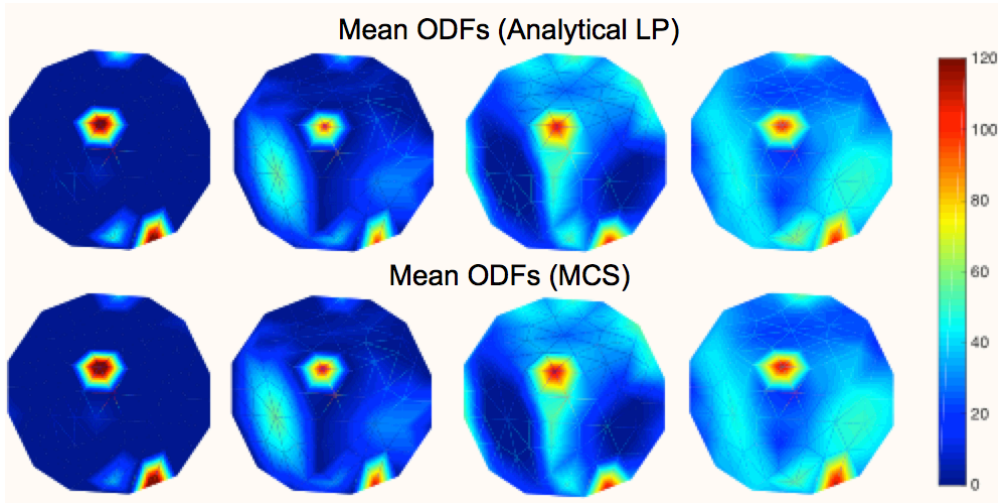


Figure 4. Examples for multiple optimum microstructures of the stochastic optimization problem

Fig. 5 implies that the variations in the optimum yield stress parameter are smaller when z is smaller. This is an expected result since z represents the variations in the ODFs. Compared to the MCS samples the best matching analytical result is provided by $z = 3.5$ condition, which was also used in the stochastic optimization.

V. Conclusion

The present work addresses a stochastic optimization problem which employs an analytical uncertainty modeling approach. The optimization problem is solved to maximize the mean value of the yield stress of a Galfenol beam under vibration tuning constraints defined for the first torsion and bending natural frequencies. We initially assumed that the probability distributions of Young's modulus and shear modulus parameters (E_1 and G_{12}) were provided. The probability distributions of these input parameters were assumed to be Gaussian with $\pm 5\%$ variations around the mean value. For vibration tuning constraints we applied the random variables transformation rule to compute the probability distributions of the first torsion and bending natural frequencies of the beam. In order to compute the probability distributions of the orientation distribution function (ODF) values we first computed the statistical properties of the compliances, S_{11} and S_{66} , using the same random variables transformation technique. We assumed that the probability distributions of the compliance parameters can be modeled with Gaussian approach since the input uncertainties are small. Next, we solved an inverse problem to identify the mean and variances of the ODF parameters. We solved the inverse design problem by implementing a linear programming (LP) problem approach since the equations to compute the compliance parameters and yield stress are linear in terms of the ODFs. We computed the values for the first $k-1$ ODF parameters, and identified the k^{th} ODF through the implementation of the volume fraction normalization constraint to the LP problem. The stochastic optimization was performed on this analytical model to find the optimal ODF solution which maximizes the mean yield stress value. We also performed another stochastic optimization which uses Monte Carlo Simulation (MCS) method to model the uncertainties. The analytical solution for uncertainty modeling not only reduced the computational time requirement for the optimization but also provided the same optimum parameters with very slight differences in yield stress and frequency parameters compared to the MCS results. A deterministic optimization was also performed to compare the optimum results with and without the effect of uncertainties. The differences on the optimum solutions of the deterministic and stochastic cases imply the necessity of considering uncertainties when modeling the materials. The multiple optimal microstructure designs were also identified by using a direct linear solver with null space approach. Finally we performed a parametric study to analyze the mathematical definition of the ODF variations in the LP problem and its effect to the optimum result. Future effort will aim to improve the analytical solution methodology so as to solve the ODF parameters without the independency assumption.

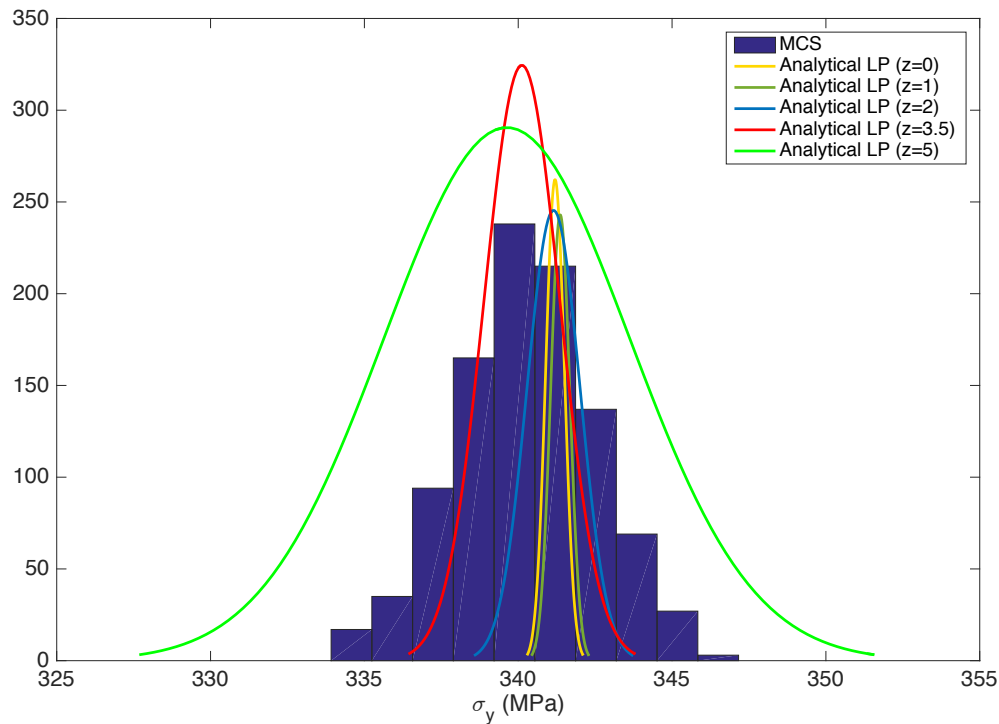


Figure 5. Yield stress distributions of the optimum microstructure design with varying z values in the analytical solution

References

- ¹Huysse, L. and Maes, M. A., "Random Field Modeling of Elastic Properties Using Homogenization," *Journal of Engineering Mechanics*, Vol. 127, No. 1, 2001, pp. 27–36.
- ²Sakata, S., Ashida, F., Kojima, T. and Zako, M., "Three-dimensional stochastic analysis using a perturbation-based homogenization method for elastic properties of composite material considering microscopic uncertainty," *International Journal of Solids and Structures*, Vol. 45, 2008, pp. 894–907.
- ³Sakata, S., Ashida, F. and Zako, M., "Kriging-based approximate stochastic homogenization analysis for composite materials," *Computer methods in applied mechanics and engineering*, Vol. 197, 2008, pp. 1953–1964.
- ⁴Clement, A., Soize, C. and Yvonnet, J., "Computational nonlinear stochastic homogenization using a nonconcurrent multiscale approach for hyperelastic heterogeneous microstructure analysis," *International Journal for Numerical Methods in Engineering*, Vol. 91, 2012, pp. 799–824.
- ⁵Clement, A., Soize, C. and Yvonnet, J., "Uncertainty quantification in computational stochastic multi-scale analysis of nonlinear elastic materials," *ICOMPUT. METHODS APPL. MECH. ENGRG*, Vol. 254, 2013, pp. 61–82.
- ⁶Creuziger, A., Syed, K. and Gnaupel-Herold, T., "Measurement of uncertainty in orientation distribution function calculations," *Scripta Materialia*, Vol. 72-73, 2014, pp. 55–58.
- ⁷Juan, L., Liu, G., Wang, H. and Ullah, A., "On the sampling of three-dimensional polycrystalline microstructures for distribution determination," *Journal of Microscopy*, Vol. 44, No. 2, 2011, pp. 214–222.
- ⁸Hiriyur, B., Waisman, H. and Deodatis, G., "Uncertainty quantification in homogenization of heterogeneous microstructures modeled by XFEM," *International Journal for Numerical Methods in Engineering*, Vol. 88, No. 3, 2011, pp. 257–278.
- ⁹Kouchmeshky, B. and Zabarvas, N., "The effect of multiple sources of uncertainty on the convex hull of material properties of polycrystals," *Computational Materials Science*, Vol. 47, No. 2, 2009, pp. 342–352.
- ¹⁰Madrid, P. J., Sulsky, D. and Lebensohn, R. A., "Uncertainty Quantification in Prediction of the In-Plane Young's Modulus of Thin Films With Fiber Texture," *Journal of Microelectromechanical Systems*, Vol. 23, No. 2, 2014, pp. 380–390.
- ¹¹Niezgoda, S. R., Yabansu, Y. and Kalidindi, S. R., "Understanding and visualizing microstructure and microstructure variance as a stochastic process," *Acta Materialia*, Vol. 59, No. 16, 2011, pp. 6387–6400.
- ¹²Acar, P. and Sundararaghavan, V., "Linear Solution Scheme for Microstructure Design with Process Constraints," *AIAA Journal*, in press, 2016.
- ¹³Acar, P. and Sundararaghavan, V., "Utilization of a Linear Solver for Multiscale Design and Optimization of Microstructures in an Airframe Panel Buckling Problem," *57th AIAA/ASCE/AHS/ASC Structures, Structural Dynamics, and Materials Conference*, AIAA-2016-0156, San Diego, CA, USA, 4-8 January 2016.
- ¹⁴Acar, P. and Sundararaghavan, V., "Utilization of a Linear Solver for Multiscale Design and Optimization of Microstructures," *AIAA Journal*, Vol. 54, No. 5, 2016, pp. 1751–1759.

¹⁵Taylor, G. I., "Plastic Strain in Metals," *Journal of the Institute of Metals*, Vol. 62, 1938, pp. 307–324.

¹⁶Kumar A., and Dawson P. R., "Computational Modeling of F.C.C. Deformation Textures over Rodrigues' Space," *Acta Materialia*, Vol. 48, No. 10, 2000, pp. 2719–2736.

¹⁷Bunge H. J., *Texture Analysis in Materials Science*, Butterworths, London, 1982.

¹⁸Wenk, H. R., *Preferred Orientation in Deformed Metals and Rocks*, Academic Press Inc., London, 1985.

¹⁹Sundararaghavan, V., and Zabarar, N., "Linear Analysis of Texture-Property Relationships Using Process-Based Representations of Rodrigues Space," *Acta Materialia*, Vol. 55, No. 5, 2007, pp. 1573–1587.

²⁰Acar, P. and Sundararaghavan, V., "Uncertainty Quantification of Microstructural Properties due to Variability in Measured Pole Figures," *Acta Materialia*, in press, 2016.

²¹Liu, R., Kumar, A., Chen, Z., Agrawal, A., Sundararaghavan, V. and Choudhary, A., "A predictive machine learning approach for microstructure optimization and materials design," *Nature Scientific Reports*, 5 (11551), 2015.

²²Ross, S. M., *Introduction to Probability Models*, 10th Edition, Elsevier, 2010.